Macromolecules

ARTICLE

pubs.acs.org/Macromolecules

Characterization and Carbonization of Highly Oriented Poly(diiododiacetylene) Nanofibers

Liang Luo,[†] Christopher Wilhelm,[†] Christopher N. Young,[‡] Clare P. Grey,[†] Gary P. Halada,[‡] Kai Xiao,[§] Ilia N. Ivanov,[§] Jane Y. Howe,[∥] David B. Geohegan,[§] and Nancy S. Goroff*[,†]

[†]Department of Chemistry, State University of New York, Stony Brook, New York 11794-3400, United States

[‡]Department of Materials Science and Engineering, State University of New York, Stony Brook, New York 11794-2275, United States

[§]Center for Nanophase Materials Sciences, Oak Ridge National Laboratory, Oak Ridge, Tennessee 37831-6030, United States

[∥]Materials Science and Technology Division, Oak Ridge National Laboratory, Oak Ridge, Tennessee 37831, United States

Supporting Information

ABSTRACT: Poly(diiododiacetylene) (PIDA), formed by the topochemical polymerization of diiodobutadiyne within host–guest cocrystals, is a conjugated polymer containing an all-carbon backbone and only iodine atom substituents. Extensive rinsing and sonication of the PIDA cocrystals in organic solvents such as methanol, THF, and chloroform yield fibrous materials with diameters as low as 10–50 nm. Raman spectroscopy and ^{13}C MAS NMR confirm that these fibers contain PIDA but that the host has been removed. Polarized Raman scattering measurements indicate that the PIDA filaments are uniaxially oriented. The PIDA nanofibers are stable at room temperature when undisturbed but become explosive under external energy such as shock or pressure. They transform to sp^2-hybridized carbon irreversibly at room temperature when irradiated with a 532 nm Raman laser beam. Under thermal conditions, the PIDA fibers start releasing iodine at 120 °C and undergo complete carbonization in 1 h by pyrolysis at 900 °C.

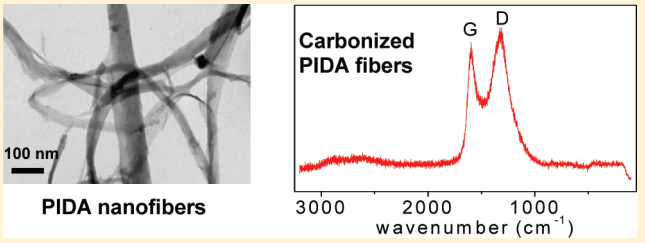

INTRODUCTION

Carbon or carbon-rich polymeric nanofibers are of broad interest for fundamental research and industrial applications in areas such as organic electronics,[1−3] hydrogen storage,[4,5] and sensors[6−8] because of their unique multifunctional properties.[9,10] Methods for preparing carbon nanofibers include catalytic decomposition of certain hydrocarbons with metal nanoparticles[11−13] and carbonization of a polymer precursor with controlled morphology.[3,14,15] However, these methods involve complicated steps for preparation and removal of catalysts or require harsh conditions such as very high temperature.[14,16] Creating 1-D carbon nanomaterials under mild conditions remains as a challenge.

Our group has recently developed a route to prepare poly(diiododiacetylene) (PIDA, **2** in Figure 1), a conjugated polymer with an all-carbon backbone and single iodine-atom substitutents.[17−19] The monomer diiodobutadiyne (**1**), aligned in a cocrystal with bis(nitrile) oxalamide host **3** or **4** by hydrogen bonds between oxalamide groups and weak Lewis acid–base interactions (halogen bonds) between nitriles and iodoalkynes, polymerizes spontaneously at room temperature in a single-crystal-to-single-crystal transformation.[18] PIDA has a nearly unadorned all-planar π-conjugated backbone and therefore offers the potential for new insights into the inherent optical and electronic properties of poly(diacetylenes) (PDAs) and other conjugated polymers. PIDA also represents a promising precursor for general PDA preparation via postpolymerization modification at the iodinated sites. More interestingly, PIDA can be considered as an ordered iodine addition product of linear carbyne. Breaking the carbon–iodine bonds of PIDA may provide a route toward structurally homogeneous and fully characterized carbon materials.

Further study of PIDA requires isolating the conjugated polymer from its hosts, which could otherwise interfere with subsequent reactions. We recently reported an efficient method to remove the host and extract PIDA from the cocrystals.[18] The pristine fully polymerized PIDA cocrystals are highly reflective and metallic in luster (e.g., cocrystals **2**·**4**, Figure 2A) because of PIDA's fully planar conjugated backbone. Extensive rinsing of the crystals in organic solvents such as methanol, THF, or chloroform results in a fine blue suspension of PIDA aggregates, fully depleted of host **4**, as judged by UV/vis absorption spectroscopy and FTIR spectroscopy.[18] TEM images of drop-cast samples from the blue suspension demonstrate that the PIDA aggregates are fibers with diameters of as low as 10–50 nm (Figure 2B). Further investigations show that high-speed centrifugation separates the suspension into a colorless supernatant layer and, interestingly, a bulk mass of solid fibers, which are still reflective and metallic in color (Figure 2C).

Received: October 11, 2010
Revised: February 25, 2011
Published: March 25, 2011

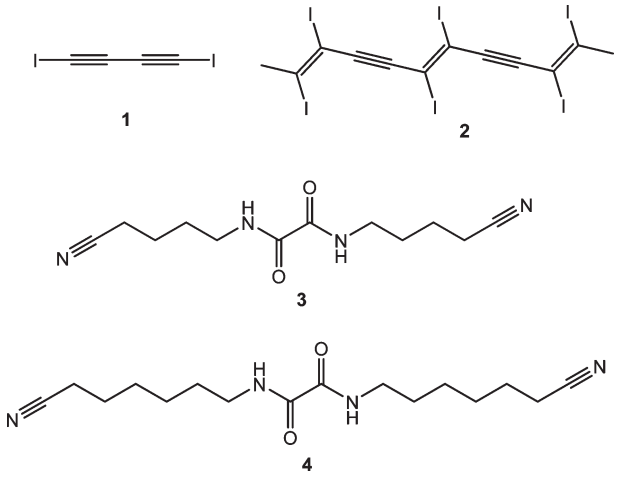

Figure 1. PIDA (**2**) can be prepared by the topochemical polymerization of diiodobutadiyne (**1**) within cocrystals **1**·**3** and **1**·**4**.

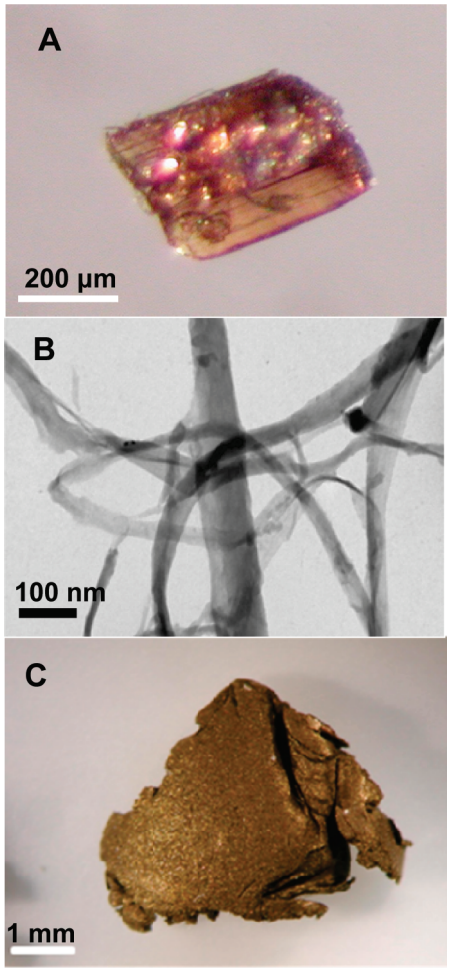

Figure 2. (A) Microscope image of cocrystal **2**·**4**. (B) TEM image of dispersed fibers, obtained from the blue suspension. (C) Bulk collection of PIDA fibers.

As in any optoelectronic material, the macroscopic properties of PIDA fibers depend on the polymer's molecular structure and

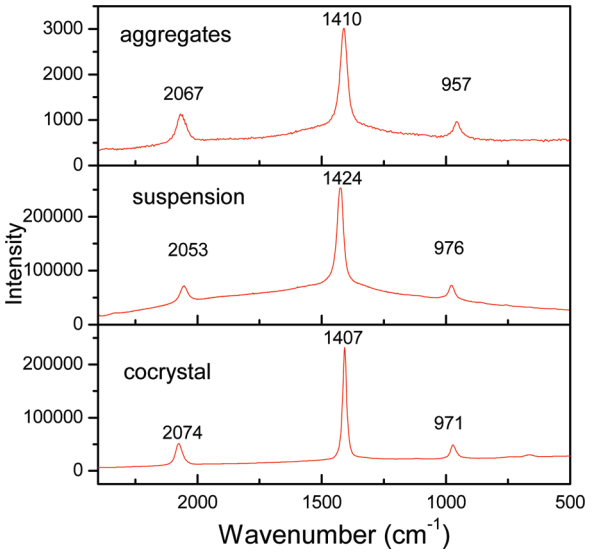

Figure 3. Raman spectra of (lower) the **2**·**4** cocrystal (pictured in Figure 2A), (middle) a PIDA suspension in THF, and (top) bulk aggregates of PIDA fibers (pictured in Figure 2C).

orientation. This paper details the characterization of the highly anisotropic PIDA nanofibers and presents initial attempts to approach carbon nanomaterials by removing iodine from PIDA. *The PIDA cocrystals are stable at room temperature, but the isolated fibers become unstable or even explosive under certain conditions such as shock, pressure, or irradiation.* Spectroscopic evidence, as described below, suggests that these exothermic reactions involve both release of iodine and cross-linking between individual polymer chains within the fiber. Thus, PIDA may readily transform to carbonaceous materials under mild conditions, in contrast to the common pyrolytic syntheses of such nanomaterials, which usually requires transition metal catalysis[20,21] and/or drastic conditions.[14,22]

RESULTS AND DISCUSSION

Raman Spectroscopy. While the morphologies of the PIDA cocrystals and isolated PIDA fibers are different, their Raman spectra are very similar. Figure 3 compares the Raman spectra of the **2**·**4** cocrystal (pictured in Figure 2A), a blue suspension of isolated PIDA, and the bulk PIDA fibers (Figure 2C), all of which were collected by reflective Raman spectroscopy using a 785 nm laser with a power of 30 mW. The Raman spectrum of the cocrystal **2**·**4** has a very high scattering intensity, attributed to the large polarizability of the poly(diacetylene) backbone.[23,24] Three major bands are visible, at 971, 1407, and 2074 cm^{-1}, corresponding to the carbon−carbon single bond, double bond, and triple bond stretches, respectively (ν(C−C), ν(C═C), ν(C≡C)). The Raman spectrum of the blue suspension is consistent with that of the cocrystals, indicating that the particles within the suspension still contain PIDA. Upon separating the solid suspension from the supernatant by high-speed centrifugation, the supernatant layer shows no Raman signal except solvent peaks. However, the isolated bulk solid gives a Raman spectrum with three major peaks, consistent with those of the PIDA cocrystals. The comparison of these Raman spectra indicates that PIDA survives the isolation process.

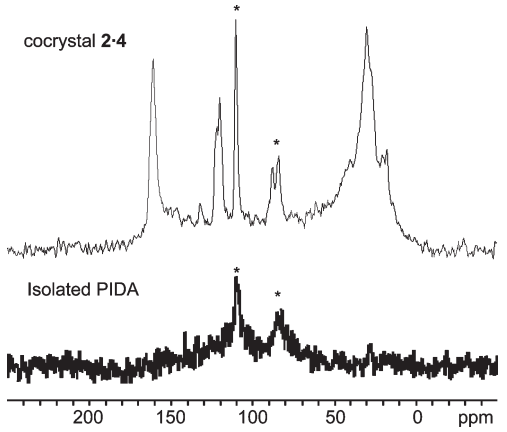

Figure 4. ^{13}C-MAS (^{1}H decoupled) NMR spectra of cocrystal **2·4** (CP MAS) and isolated PIDA (direct excitation). The asterisks indicate resonances assigned to the PIDA carbon atoms.

The Raman scattering intensity of the PIDA fibers is much weaker than those of the suspension or the cocrystals, a difference that may be attributed to the rough surface of the bulk PIDA fibers, or possibly to decomposition of isolated PIDA under laser irradiation. In fact, all the Raman spectra must be collected at 10% of standard laser power (2.5 mW). At greater power, a broad fluorescent background obstructs the Raman scattering signal,[25] and prolonged irradiation leads to visible destruction of the sample, resulting in a material with no discernible Raman scattering. PIDA's significant fluorescence signal at high laser power is consistent with a large multiphoton absorption cross section, something that has been observed in other polydiacetylenes.[26−28]

^{13}C MAS NMR. Obtaining a solid-state ^{13}C MAS NMR spectrum of isolated PIDA proved difficult. The material contains no hydrogen atoms, and therefore the ^{13}C NMR data must be collected through direct methods, a slow process because of the long nuclear spin−lattice relaxation times. More significantly, our efforts to collect data on these samples revealed that *isolated PIDA is a shock explosive*. Two different samples exploded while in a spinning rotor, and a third sample exploded as it was being packed into the rotor. The soot showed evidence of formed molecular iodine (I_2), as described below, but has not been studied further. Diluting fresh samples of isolated PIDA with the salt sodium nitrate allowed us to collect data without sample decomposition.[29] Although the Larmor frequencies of carbon and sodium are close in value (176 and 185 MHz, respectively, at a field strength of 16.4 T), the use of high-field NMR allows for adequate resolution of the ^{13}C NMR spectrum. However, the small sample size and direct NMR sampling method contribute to the poor signal-to-noise ratio that is observed in the spectrum. The resulting ^{13}C NMR spectrum (Figure 4) shows only two peaks, at 82 and 110 ppm, attributed to the α-carbon (sp^2) and β-carbon (sp) of PIDA, but with no peak corresponding to the host, consistent with successful isolation of solid PIDA.[30] Furthermore, the observed chemical shifts indicate that the structural integrity of the polymer is maintained throughout the isolation process. The increased breadth of the peaks, however, suggests that aggregation of the polymer strands changes their electronic and magnetic environment, consistent with the observation of a long-wavelength UV/vis absorption in the PIDA aggregates[18] that is not present in the cocrystals.

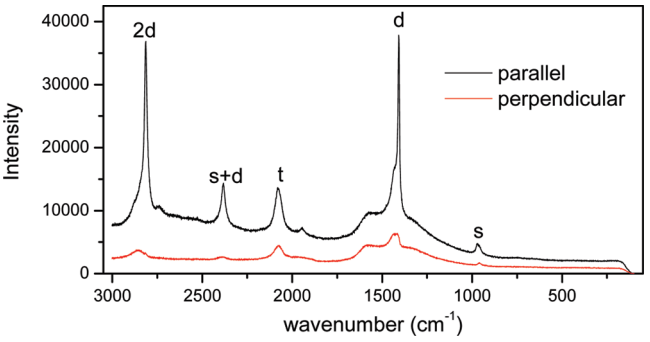

Figure 5. Raman spectra of a PIDA fiber with fiber long axes aligned parallel (black trace) and perpendicular (red trace) to Raman polarization.

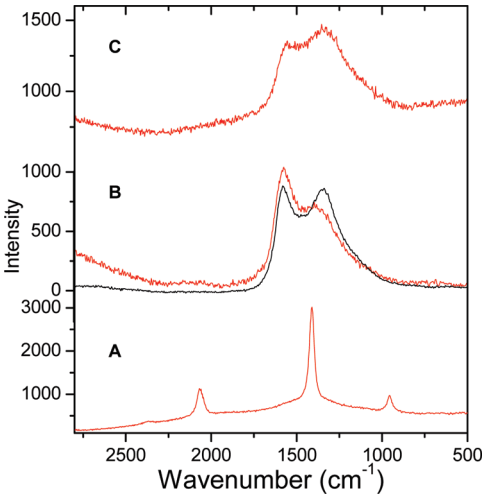

Figure 6. Raman spectra of PIDA fibers at different laser wavelengths. (A) Initial measurement with irradiation at 785 nm. (B) Measurement with irradiation at 532 nm (red), shown with overlay of the spectrum for commercial graphite (black). (C) Repeat measurement at 785 nm. Each spectrum was measured at the same spot on the sample.

Polarized Raman Spectroscopy. To identify the organization of PIDA within the nanofibers, we have employed polarized Raman spectroscopy. In general, alignment of the polarization direction of the irradiating laser beam with the long axis of a conjugated polymer chain should maximize the polarized Raman scattering intensity. Compared with the standard Raman spectrum of the PIDA fibers shown in Figure 3, the polarized Raman (Figure 5) of single PIDA fibers looks similar but includes two new peaks, at 2388 and 2817 cm^{-1}, in addition to the previously observed ν(C−C), ν(C═C), and ν(C≡C) stretches. The peak at 2388 cm^{-1} corresponds to a combination mode of the single- and double-bond stretches (s+d). The peak at 2817 cm^{-1} corresponds to an overtone of the double-bond stretch (2d). These two peaks are easily visible in the parallel-polarized Raman spectrum of aligned PIDA fibers but very weak both in the perpendicularly polarized Raman spectrum and in the standard unpolarized Raman spectrum of PIDA (Figure S1, Supporting Information).

The two polarized Raman spectra demonstrate the anisotropic scattering of PIDA. When the fiber is aligned parallel to the

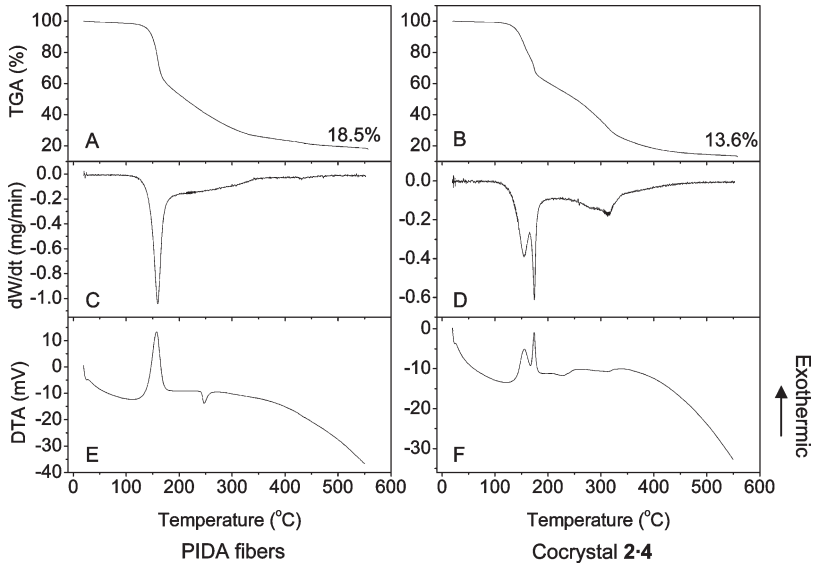

Figure 7. Thermal analysis of PIDA fibers and PIDA cocrystal **2·4**: (A, B) TGA of PIDA fibers and cocrystals; (C, D) the related weight loss rates; (E, F) DTA of PIDA fibers and cocrystals.

polarization direction of the laser beam, the scattering intensity of the fiber is much higher than when the fiber is aligned perpendicular to the Raman polarization. Comparing the d-band in the two spectra measured at the same spot on a PIDA fiber, the ratio of intensities is approximately 6:1, indicating that the fiber is highly anisotropic and the polymers within the fiber are oriented uniaxially.[31,32] In addition, Raman mapping allows further characterization of the orientation and morphology of the PIDA fiber (Figure S2, Supporting Information). The detailed map shows that the Raman intensities are homogeneous across the fiber, indicating that the polymer chains within the fiber are all parallel to one another and to the long axis of the fiber.

Carbonization of PIDA Fibers. The PIDA fibers are stable at room temperature when undisturbed. However, as described above, PIDA fibers can explode under external energy such as shock or pressure. Rinsing the soot that results from such an explosion yields a pink chloroform solution, with absorption maximum centered at 505 nm. Adding $Na_2S_2O_3$ to the solution quenches the color, indicating that molecular iodine is formed during the explosion.

Carbonization of PIDA fibers can also be induced by visible-wavelength laser irradiation at room temperature. When the Raman spectrum of isolated PIDA is measured using a 532 nm laser, instead of 785 nm irradiation, the resulting spectrum looks very different, with broad peaks at ~1600 and 1380 cm^{-1}, consistent with sp^2-hybridized carbon, as shown in Figure 6. Irradiating the same sample spot again at 785 nm, the Raman scattering signal does not revert to the previously observed signal for PIDA, indicating that the 532 nm laser irradiation induces an irreversible structural transformation. The power settings for the 532 and 785 nm lasers in these experiments are approximately the same (about 2.5 mW at the sample), suggesting that the change in frequency is responsible for this difference in behavior.

The mechanism for this transformation is not clear. Isolated PIDA fibers are stable under ambient light but react quickly under visible laser irradiation, consistent with multiphoton absorption. The polymer chains are closely aggregated within the PIDA fibers, so the transformation of PIDA to sp^2-hybridized materials

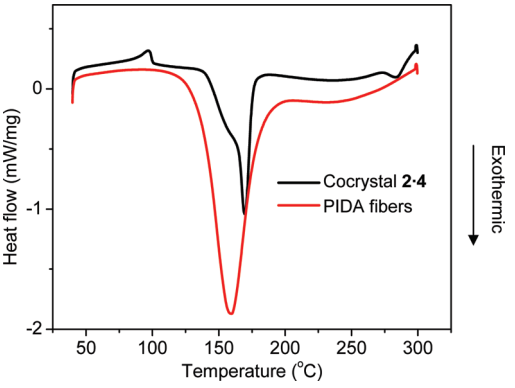

Figure 8. DSC plots for PIDA fibers and PIDA cocrystal **2·4**.

may coincide with cross-linking of the carbon backbones, either before or after photophysical or thermal loss of iodine.

The thermal degradation behavior of PIDA can be characterized by thermogravimetric analysis (TGA) and differential thermal analysis (DTA), as shown in Figure 7. The TGA data for isolated PIDA fibers (Figure 7A) illustrate weight loss starting at ~120 °C, with greatest loss in the temperature range from 140 to 170 °C, and a total weight loss of 81.5% at 550 °C, compared to an iodine content of 84.1 mass %. The rate of weight loss, shown in Figure 7C, reaches a maximum value at 157 °C, most easily visualized by the exothermic peak in the DTA scan (Figure 7E). This result suggests that PIDA readily decomposes to carbon plus iodine at relatively low temperatures. In comparison, the thermal analysis of PIDA cocrystal **2·4** (Figure 7B,D,F) exhibits a similar exothermic release in a temperature range of 150−170 °C, followed by another smaller weight loss from 250 to 320 °C. Comparison of the TGA spectra for cocrystal **2·4** and host **4** alone (Figure S3, Supporting Information) suggests that the weight loss in the higher temperature range is caused by evaporation of the host, while the initial weight loss corresponds to loss of iodine. As in the isolated fibers, the PIDA cocrystals continue to lose mass above this temperature range, but at a

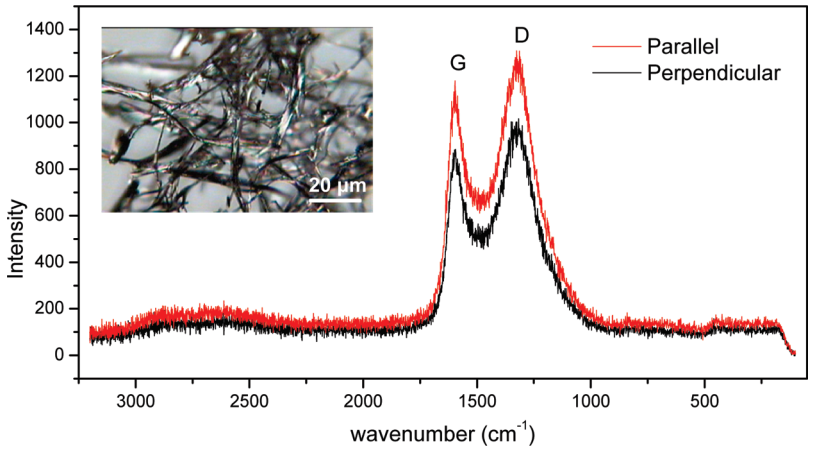

Figure 9. Polarized Raman measurements of annealed PIDA fibers (inset) in geometries perpendicular (A) and parallel (B) to Raman polarization.

much slower rate, until the remaining mass (13.6%) corresponds closely to the theoretical value for only the carbon of the polymer (10.6%), at ~550 °C (see Table S1, Supporting Information).[33]

DSC analysis of PIDA cocrystal **2·4** and the PIDA fibers further reveals the exothermicity of the carbonization process. The DSC trace for PIDA cocrystal **2·4** shows an endothermic peak at 98 °C, which is consistent with the melting point of host **4**. The strong exothermic peak in the spectrum at 170 °C, with a shoulder starting from 140 °C, indicates that the weight loss in this range (shown in TGA) is highly exothermic. The thermolysis of PIDA fibers shows no endothermic peak but a stronger exothermic peak at 159 °C compared with the cocrystals, even after correction for the mass of the host in the cocrystals (see Figure S4, Supporting Information). This result suggests that iodine dissociation is more favorable in the isolated PIDA fibers, consistent with simultaneous exothermic interchain cross-linking.

To carbonize PIDA completely, the isolated fibers were annealed at 900 °C under an argon atmosphere for 1 h. The resulting material is shiny and fibrous in appearance, as shown in the inset in Figure 9. According to energy dispersive spectroscopy (EDS) measurements, the iodine of PIDA is completely removed as a result of the pyrolysis (Figure S5, Supporting Information). Polarized Raman measurements of the annealed PIDA fibers indicate that the material has been completely converted to sp^2-hybridized carbon material. The peak at 1583 cm^{-1} is consistent with the G band of graphitic carbon, and the broader peak centered around 1380 cm^{-1} corresponds to the disordered sp^2-hybridized carbon D band.[34,35] The polarized Raman spectra of an annealed PIDA fiber, taken with the fiber either parallel or perpendicular to the Raman polarization, are almost identical (Figure 9), indicating the presence of a new isotropic material upon annealing.

CONCLUSION

The extraction of PIDA from host−guest cocrystals yields highly oriented fibers of polymer aggregates. PIDA in these fibers can be transformed to sp^2-hybridized carbon by irradiation with a 532 nm Raman laser. Thermogravimetric analysis suggests that PIDA loses almost all its iodine below 550 °C, while complete carbonization takes place with pyrolysis at 900 °C for 1 h. These facile transformations suggest that dissociation of the carbon−iodine bonds in PIDA requires relatively little energy. We will continue to explore methods to achieve complete dissociation of iodine from PIDA under mild conditions.

ASSOCIATED CONTENT

Supporting Information. Complete experimental information, including preparation of PIDA fibers and details of instrumental methods, additional TGA spectra, Raman mapping images, and EDS spectrum of carbonized fibers. This material is available free of charge via the Internet at http://pubs.acs.org.

AUTHOR INFORMATION

Corresponding Author
*E-mail: nancy.goroff@stonybrook.edu.

ACKNOWLEDGMENT

We thank the National Science Foundation (CHE-9984937, CHE-0446749, CHE-0453334, and DMR-0804737) for support of this research. A portion of this research was conducted at the Center for Nanophase Materials Sciences and the SHaRE User Facility, which is sponsored at Oak Ridge National Laboratory by the Division of Scientific User Facilities, U.S. Department of Energy (CNMS2009-017). We also thank Allison L. Stelling and Prof. Peter J. Tonge of Stony Brook University for help with Raman of the suspension, as well as Heng Zhang, Dr. Feng Zuo, and Prof. Lorraine F. Francis of University of Minnesota for help with TGA and DSC experiments.

REFERENCES

(1) Chung, D. D. L. *Carbon* **2001**, *39*, 279–285.
(2) Avouris, P. *Acc. Chem. Res.* **2002**, *35*, 1026–1034.
(3) Feng, X. L.; Liang, Y. Y.; Zhi, L. J.; Thomas, A.; Wu, D. Q.; Lieberwirth, I.; Kolb, U.; Mullen, K. *Adv. Funct. Mater.* **2009**, *19*, 2125–2129.
(4) Chambers, A.; Park, C.; Baker, R. T. K.; Rodriguez, N. M. *J. Phys. Chem. B* **1998**, *102*, 4253–4256.
(5) Park, C.; Anderson, P. E.; Chambers, A.; Tan, C. D.; Hidalgo, R.; Rodriguez, N. M. *J. Phys. Chem. B* **1999**, *103*, 10572–10581.
(6) Kong, J.; Franklin, N. R.; Zhou, C. W.; Chapline, M. G.; Peng, S.; Cho, K. J.; Dai, H. J. *Science* **2000**, *287*, 622–625.
(7) Li, J.; Lu, Y. J.; Ye, Q.; Cinke, M.; Han, J.; Meyyappan, M. *Nano Lett.* **2003**, *3*, 929–933.
(8) Gill, I.; Ballesteros, A. *Angew. Chem., Int. Ed.* **2003**, *42*, 3264–3267.

(9) De Jong, K. P.; Geus, J. W. *Catal. Rev.—Sci. Eng.* **2000**, *42*, 481–510.
(10) Endo, M.; Kim, Y. A.; Hayashi, T.; Nishimura, K.; Matusita, T.; Miyashita, K.; Dresselhaus, M. S. *Carbon* **2001**, *39*, 1287–1297.
(11) Iijima, S. *Nature* **1991**, *354*, 56–58.
(12) Rodriguez, N. M. *J. Mater. Res.* **1993**, *8*, 3233–3250.
(13) Iyer, V. S.; Vollhardt, K. P. C.; Wilhelm, R. *Angew. Chem., Int. Ed.* **2003**, *42*, 4379–4383.
(14) Kyotani, M.; Matsushita, S.; Nagai, T.; Matsui, Y.; Shimomura, M.; Kaito, A.; Akagi, K. *J. Am. Chem. Soc.* **2008**, *130*, 10880–10881.
(15) Laskoski, M.; Steffen, W.; Morton, J. G. M.; Smith, M. D.; Bunz, U. H. F. *J. Am. Chem. Soc.* **2002**, *124*, 13814–13818.
(16) Partouche, E.; Margel, S. *Carbon* **2008**, *46*, 796–805.
(17) Sun, A. W.; Lauher, J. W.; Goroff, N. S. *Science* **2006**, *312*, 1030–1034.
(18) Luo, L.; Wilhelm, C.; Sun, A.; Grey, C. P.; Lauher, J. W.; Goroff, N. S. *J. Am. Chem. Soc.* **2008**, *130*, 7702–7709.
(19) Wilhelm, C.; Boyd, S. A.; Chawda, S.; Fowler, F. W.; Goroff, N. S.; Halada, G. P.; Grey, C. P.; Lauher, J. W.; Luo, L.; Martin, C. D.; Parise, J. B.; Tarabre, C.; Webb, J. A. *J. Am. Chem. Soc.* **2008**, *130*, 4415–4420.
(20) Guo, T.; Nikolaev, P.; Thess, A.; Colbert, D. T.; Smalley, R. E. *Chem. Phys. Lett.* **1995**, *243*, 49–54.
(21) Benito, A. M.; Maniette, Y.; Munoz, E.; Martinez, M. T. *Carbon* **1998**, *36*, 681–683.
(22) Oberlin, A. *Carbon* **1984**, *22*, 521–541.
(23) Horvath, A.; Weiser, G.; LapersonneMeyer, C.; Schott, M.; Spagnoli, S. *Phys. Rev. B* **1996**, *53*, 13507–13514.
(24) Weiser, G. *Phys. Rev. B* **1992**, *45*, 14076–14085.
(25) Kim, H.; Kosuda, K. M.; Van Duyne, R. P.; Stair, P. C. *Chem. Soc. Rev.* **2010**, *39*, 4820–4844.
(26) Lemoigne, J.; Kajzar, F.; Thierry, A. *Macromolecules* **1991**, *24*, 2622–2628.
(27) Guo, D.; Mazumdar, S.; Dixit, S. N.; Kajzar, F.; Jarka, F.; Kawabe, Y.; Peyghambarian, N. *Phys. Rev. B* **1993**, *48*, 1433–1459.
(28) Lawrence, B.; Torruellas, W. E.; Cha, M.; Sundheimer, M. L.; Stegeman, G. I.; Meth, J.; Etemad, S.; Baker, G. *Phys. Rev. Lett.* **1994**, *73*, 597–600.
(29) Note: although we did not encounter any problems in our experiments when using this diluent, we do not recommend mixing the diluent sodium nitrate with a shock explosive.
(30) Because the host contains multiple protonated carbons, $^{1}H/^{13}C$ cross-polarization experiments could be performed for the cocrystal, explaining the much better signal-to-noise of the ^{13}C NMR spectrum of the cocrystal in comparison to the isolated PIDA.
(31) Frisk, S.; Ikeda, R. M.; Chase, D. B.; Kennedy, A.; Rabolt, J. F. *Macromolecules* **2004**, *37*, 6027–6036.
(32) Song, K.; Rabolt, J. F. *Macromolecules* **2001**, *34*, 1650–1654.
(33) The theoretical iodine compostion of PIDA fiber is 84.1%. For cocrystals, assuming all the host has been evaporated at 550 °C. The theoretical composition of the host is 33.6%, and that of iodine is 55.8%.
(34) Ferrari, A. C.; Robertson, J. *Phys. Rev. B* **2000**, *61*, 14095–14107.
(35) Ferrari, A. C.; Meyer, J. C.; Scardaci, V.; Casiraghi, C.; Lazzeri, M.; Mauri, F.; Piscanec, S.; Jiang, D.; Novoselov, K. S.; Roth, S.; Geim, A. K. *Phys. Rev. Lett.* **2006**.